Solid State Phenomena Vols. 121-123 (2007) pp. 933-937
online at http://www.scientific.net
© (2007) Trans Tech Publications, Switzerland

Photoluminescence and Raman Studies on Boron-doped Nanocrystalline Si:H Thin Films

H. Chen[1, a], W. Z. Shen[1,b, ¶] and W. S. Wei[2]

[1]Laboratory of Condensed Matter Spectroscopy and Opto-Electronic Physics, Department of Physics, Shanghai Jiao Tong University, 1954 Hua Shan Road, Shanghai 200030, P. R. China

[2]School of Physics and Information, Wenzhou University, Wenzhou, Zhejiang 325027, P. R. China

[a]chenhong@sjtu.edu.cn, [b]wzshen@sjtu.edu.cn

[¶]Corresponding author

Keywords: boron-doped, hydrogenated nanocrystalline silicon, photoluminescence, Raman.

Abstract. We report on room-temperature visible photoluminescence (PL) of B-doped hydrogenated nanocrystalline Si (nc-Si:H) thin films grown by plasma enhanced chemical vapor deposition. It is found that with increasing the boron doing ratio, the PL peak energy blue shifts while the PL intensity first increases and then decreases. The PL profiles can be well reproduced by using the model of Islam and Kumar [J. Appl. Phys. **93**, 1753 (2003)] which incorporates the effects of quantum confinement and localized surface states, together with a log-normal rather than normal crystallite size distribution. The yielded microstructural information is in good agreement with the Raman analysis, revealing that B doping tends to reduce the size of Si nanocrystals and the PL intensity is jointly determined by the amount of amorphous Si:H phase and the fraction of B-doped Si nanocrystals. These results also provide implications to realize control of PL properties of nc-Si:H by B doping under optimized growth conditions.

1. Introduction

Since the observation of efficient visible photoluminescence (PL) from porous Si [1], interest in optical properties of various Si nanostructures (NSs) where Si nanocrystals are embedded in matrix materials such as SiO_2 [2,3] and amorphous Si:H (a-Si:H) [4] has been stimulated by their potential applications to optoelectronic devices. The role of impurity doping on PL properties of Si NSs is important from the viewpoints of both fundamental physics and future applications, thus relevant studies of impurity-doped Si NSs are indispensable. However, little is known about the influence of *p*-type impurity doping on PL properties of Si nanocrystals embedded in a-Si:H so far, although results of those (both *n*-type and *p*-type doped) embedded in SiO_2 have been intensively investigated [2,3]. Furthermore, the PL mechanism in the Si NSs is not yet fully understood in spite of many models proposed to

All rights reserved. No part of contents of this paper may be reproduced or transmitted in any form or by any means without the written permission of the publisher: Trans Tech Publications Ltd, Switzerland, www.ttp.net. (ID: 218.80.66.85-25/10/06,02:08:25)

explain the light emission [5–7].

In this article, we report on room-temperature visible PL and Raman properties of boron-doped hydrogenated nanocrystalline Si (nc-Si:H) thin films (where Si nanocrystals, i.e., grains, are embedded in an a-Si:H matrix), which were grown by plasma enhanced chemical vapor deposition (PECVD). Unlike B-doped Si nanocrystals embedded in SiO_2 [3], the PL peak energy of the B-doped nc-Si:H is found to be sensitive to the boron doping ratio (C_B) and the PL intensity first increases and then decreases with increasing C_B. The microstructural information and PL mechanism are also revealed through the PL and Raman analyses.

2. Experimental details

The studied *p*-type nc-Si:H thin films were prepared in a radio frequency (rf) (13.56 MHz) capacitive coupled PECVD system from silane (SiH_4) and hydrogen (H_2) on undoped crystalline Si (111) substrates at a temperature of 250 ºC. Diborane (B_2H_6) was used as dopant gas, and hydrogen dilution ratio [$H_2/(SiH_4+H_2)$] remained constant of 99% during the deposition. C_B (=B_2H_6/SiH_4) were 1%, 5%, and 10% for the three typical nc-Si:H samples with film thickness of about 2μm. The total pressure of reactive gases was 0.70Torr. Unpolarized Raman scattering (in backscattering configuration) and PL spectra were performed on the same sample spots at room temperature on a Jobin Yvon LabRAM HR 800 UV Micro-Raman spectrometer using 514.5nm line from an Ar^+ laser. Care was taken to avoid sample heating due to the incident laser beam.

3. Results and discussion

Fig 1(a) shows the room-temperature experimental (open points) PL spectra of the B-doped nc-Si:H with three different C_B. All the PL spectra are normalized at their maximum intensities and shifted vertically for clarity. It is found that when C_B increases from 1% to 10%, the PL peak energy blue shifts from 1.56eV to 2.01eV and the PL intensity first increases and then decreases. The PL profiles (open points) can be well reproduced by using the model (solid curves) proposed by Islam and Kumar (denoted as I-K model hereinafter) [7] which incorporates the effects of quantum confinement (QC) and localized surface states (LSS), together with a log-normal rather than normal distribution of grain sizes. (The normal distribution case is excluded here for yielding unreasonable fitting results.) According to the I-K model, the expression for PL intensity $I(\Delta E)$ in the case of log-normal crystallite size distribution is

$$I(\Delta E) = I_0 \frac{(C/\Delta E)^{(5-\alpha+n)/n}}{nC\sigma} \exp\left[\frac{-\{[\ln(C/\Delta E)]^{1/n} - \ln(L_0)\}^2}{2\sigma^2}\right], \quad (1)$$

with ΔE the amount of band gap widening due to QC effect (QCE), I_0 a proportional constant, L_0 approximately the average grain size, σ/L_0 describing the size dispersion, and the other parameters of the same physical significance as in Eq. (12) of Ref. [7]. During the fitting, we only let I_0, σ, and L_0 vary, and adopt the same values of the other fitting parameters as in Ref. [7]. The fitted results are given in Fig. 2, indicating that the average grain size decreases with increasing C_B.

It is worth noting that the PL mechanism in various Si NSs is not yet fully understood so far, although many explanations have been proposed [5–7]. To date, QCE in Si NSs has been widely accepted to open up the band gap as well as relax the selection rules for radiative transitions [7], giving rise to visible PL for nanocrystallite size below ~ 5nm. However, localized surface states or defects, such as hydrides or Si dangling bonds around nanocrystals also influence the PL peak energy and profile. In addition, the surface to volume ratio increases as the grain size decreases, the influence of surface states on the PL from smaller nanocrystals will be highly enhanced [7]. The fact that the QC model without considering the effect of LSS [6] alone cannot well reproduce the experimental PL spectra partially rationalizes the usage of the I-K model for the B-doped nc-Si:H samples.

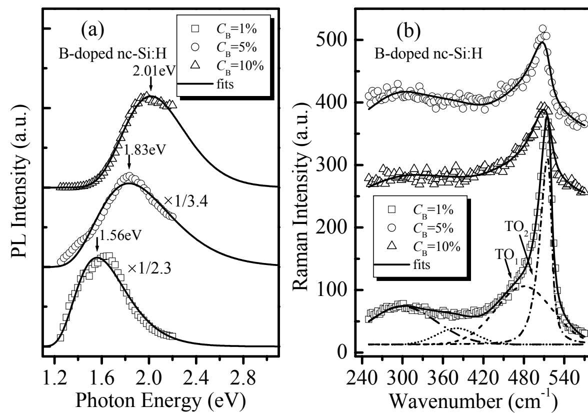

Fig. 1. (a) Room-temperature experimental (open points) and calculated (solid curves) PL and (b) Raman spectra of B-doped nc-Si:H thin films deposited at different doping ratios C_B. All the PL spectra are normalized at their maximum intensities and shifted vertically for clarity, while all the Raman spectra are as-measured without any vertical shift.

In order to get more evidence for the reasonable employment of the I-K model and gain deeper insight into the PL mechanism in B-doped nc-Si:H, we resort to the Raman analysis. Fig. 1(b) shows the corresponding experimental (open points) as-measured Raman spectra without any vertical shift. Notice that their baselines are strikingly high due to the disorder (or amorphous Si or a-Si:H) background for the three samples, especially for C_B=5% and 10%. As displayed typically for the sample of C_B=1% in Fig. 1(b), We decompose the experimental data into three Gaussian phonon bands [i.e., longitudinal acoustic band centered at 300cm^{-1}, longitudinal optical band at 380cm^{-1}, and transverse optical (TO_1) band at 480cm^{-1}] from the amorphous Si contribution, and one asymmetric transverse optical (TO_2) band at ~520cm^{-1} from the crystalline Si contribution calculated by the strain-incorporated three-dimensional phonon confinement model [8], after subtracting a constant background parameter *bg*. The calculated results (solid curves) via least-squares fit agree well with the experimental ones. The crystallinity X_c can be obtained by using $X_c = I_{TO_2}/(I_{TO_2} + \gamma I_{TO_1})$, where $\gamma(L_0) = 0.1 + \exp(-L_0/25)$ with L_0 the average grain size in units of nm, and I_{TO_1} and I_{TO_2} are integrated intensities of TO_1 and TO_2 modes, respectively [9]. The resulting L_0, *bg*, and X_c are given in Fig. 2.

It is clear from Fig. 2 (a) that the average grain sizes L_0 deduced from Raman coincide well with those from PL within the relative error of ~5%, directly verifying the reliability of the I-K model used here. In other words, the PL peak energy is mainly attributed to the QCE in the B-doped nc-Si:H. The background parameter *bg* which reflects the degree of disorder is indicative of the relative volume fraction of amorphous Si or a-Si:H. Thus, the larger the *bg*,

the more the disorder and the less the crystallinity, as demonstrated by the *bg* and X_c data in Fig. 2 (b). In addition, size dispersion also reflects the disorder to some extent. The variation of σ/L_0 [Fig. 2 (b)] with C_B deduced from the PL analysis is consistent with those of *bg* and X_c, confirming the consistency between the PL and Raman analyses. Of particular interest is that the larger the *bg*, the larger the PL intensity proportional constant I_0, as shown in Fig. 2(b). Since the B-doped nc-Si:H samples were deposited in highly hydrogen diluted silane by PECVD, the Si nanocrystals are generally surrounded by a-Si:H layers. Therefore, the a-Si:H surfaces of the grains contribute positively to the PL intensity, as implied by the correlation between *bg* and I_0. This highlights the importance of the LSS involved in PL. The PL process in the B-doped nc-Si:H thus can be understood in terms of the I-K model as follows: the photoexcitation occurs inside the Si nanocrystals, and then a fraction of photocarriers relax nonradiatively to the surface states; subsequently, the relaxed carriers recombine to ground states radiatively giving PL.

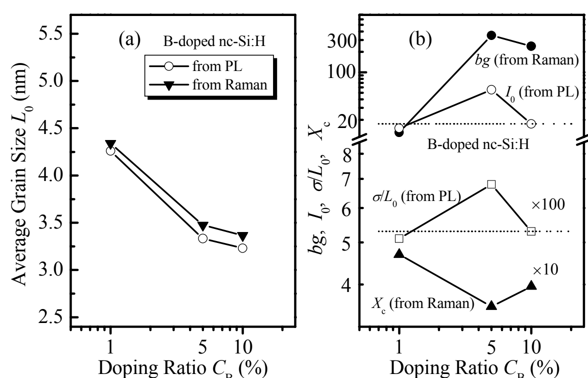

Fig. 2. (a) The average grain size L_0, and (b) background parameter *bg*, proportional constant I_0, size dispersion σ/L_0, crystallinity X_c deduced from the PL and Raman analyses for the B-doped nc-Si:H. The dotted horizontal lines are drawn as guides to the eye.

Finally, comparison is made between the roles of boron doping on the PL properties of above Si nanocrystals embedded in a-Si:H and those embedded in SiO_2 in the literature. In the latter case [3], the increase of boron doping does not affect the PL peak energy but leads to PL quenching. In contrast, in B-doped nc-Si:H, the PL peak energy blue shifts and the PL intensity first increases and then decreases with the increase of the boron doping ratio C_B. Conductivity measurements show that the dark conductivity of these nc-Si:H increases with increasing C_B, revealing that more B atoms are incorporated into the nc-Si:H with the increase of C_B. Since the PL peak energy is mainly determined by the grain size within the framework of QCE, the difference in the variation of grain size caused by boron doping is due to the difference between the two growth methods, i.e., the rf cosputtering [3] and the chemical vapor deposition (CVD). In the rf cosputtering method, the grain size is controlled by changing the number of Si chips or the annealing temperature, and is almost independent of boron doping [3]. Whereas the boron doping tends to reduce the grain size and induce disorder in nc-Si:H grown by PECVD; similar phenomenon has also been observed in the case of hot-wire CVD [10]. On the other hand, the B atoms are believed to exist mainly in the amorphous interface region among Si grains for $C_B \leq 5\%$, since the PL intensity is not reduced but even enhanced when C_B increases from 1% to 5%. When C_B=10%, the PL intensity reduces a lot as compared to those of C_B=1% and 5%, suggesting that more B atoms have been doped into the Si grains of at C_B=10%. The relevant I_0 for C_B=10% is only slightly larger than that for C_B=1% partly because

of more B atoms doped into Si grains, if we expect that I_0 is roughly proportional to bg. In other words, the PL intensity of the B-doped nc-Si:H is dependent on both the amount of a-Si:H phase and the degree of quenching caused by boron doped into the Si grains.

4. Conclusions

In summary, we have investigated the room-temperature visible PL and Raman spectra of B-doped nc-Si:H thin films grown by PECVD. The PL can be well explained by using the I-K model with considering a log-normal crystallite size distribution. The yielded microstructural information is consistent with the Raman analysis, revealing that B doping tends to reduce the average grain size of nc-Si:H. The blue shift of the PL peak with the variation of B doping ratio is mainly ascribed to QCE, and the PL intensity is jointly determined by the amount of a-Si:H component and the fraction of B-doped Si grains within the nc-Si:H. These results have implications to control the PL properties of nc-Si:H by B doping for future optoelectronic applications.

Acknowledgements

This work was supported in part by the Natural Science Foundation of China under contract No. 10125416, and Shanghai municipal major project of 03DJ14003.

References

1. L. T. Canham, Appl. Phys. Lett. **57**, 1046 (1990).
2. M. Fujii, A. Mimura, S. Hayashi, Y. Yamamoto, and K. Murakami, Phys. Rev. Lett. **89**, 206805 (2002).
3. M. Fujii, S. Hayashi, and K. Yamamoto, J. Appl. Phys. **83**, 7953 (1998).
4. H. Chen and W. Z. Shen, J. Appl. Phys. **96**, 1024 (2004).
5. A. G. Cullis, L. T. Canham, and P. D. J. Calcott, J. Appl. Phys. **82**, 909 (1997).
6. P. F. Trwoga, A. J. Kenyon, and C. W. Pitt, J. Appl. Phys. **83**, 3789 (1998).
7. M. N. Islam and S. Kumar, J. Appl. Phys. **93**, 1753 (2003).
8. M. Yang, D. M. Huang, P. H. Hao, F. L. Zhang, X. Y. Hou, and X. Wang, J. Appl. Phys. **75**, 651 (1994).
9. E. Bustarret, M. A. Hachicha, and M. Brunel, Appl. Phys. Lett. **52**, 1675 (1988).
10. S. R. Jadkar, J. V. Sali, M. G. Takwale, D. V. Musale, and S. T. Kshirsagar, Sol. Energy Mater. Sol. Cells **64**, 333 (2000).